

Optimization of the tunability of barium strontium titanate films via epitaxial stresses

Z.-G. Ban and S. P. Alpay^{a)}

Department of Metallurgy and Materials Engineering and Institute of Materials Science, University of Connecticut, Storrs, Connecticut 06269

(Received 2 July 2002; accepted 6 October 2002)

The tunability of epitaxial barium strontium titanate films is analyzed theoretically using a phenomenological model. The relative dielectric constant of $\text{Ba}_{0.5}\text{Sr}_{0.5}\text{TiO}_3$ (BST 50/50) films as a function of the applied external electric field is calculated and an electric field–misfit strain phase diagram is developed to assist in the interpretation of the behavior. On the basis of these results, the tunability of BST 50/50 films as a function of the misfit strain is provided and compared with the experimental data in the literature. Analysis shows that a high tunability can be achieved by adjusting the misfit strain especially in the vicinity of a structural phase transformation. The misfit strain in epitaxial films can be controlled with the selection of a substrate material or variations in the film thickness. The film thickness dependence is due to misfit dislocation formation at the film growth temperature. A critical thickness to attain the maximum tunability can be defined for BST 50/50 films on MgO (~90 nm) and LaAlO_3 (~120 nm) substrates. It is suggested that the selection of the substrate and/or the film thickness can be chosen as design parameters to manipulate the strain state in the film to achieve optimum tunability. © 2003 American Institute of Physics.

[DOI: 10.1063/1.1524310]

I. INTRODUCTION

Thin films of barium strontium titanate ($\text{Ba}_x\text{Sr}_{1-x}\text{TiO}_3$, (BST) have long been recognized as the potential candidates for applications such as storage capacitor dielectrics for the next generation dynamic random access memories as well as variable elements in the tunable microwave devices.^{1–6} These applications rely on the properties of BST films, such as a high dielectric permittivity, reasonably low dielectric loss, and high tunability. The tunability (i.e., the degree of variation in the dielectric constant as a function of the applied electric field) is one of key design parameters of tunable microwave devices. Ideally, a large tunability accompanied by a small dielectric loss is desired.

There has been a great deal of research in the field of ferroelectric thin films, the primary objective of which has been to reliably reproduce the properties of bulk ceramics or single crystals in thin film form for device applications. However, compared to their bulk or single crystal counterparts, generally inferior electrical and electromechanical properties are observed in ferroelectric thin films. The reason for this is believed to be due to compositional and microstructural inhomogeneities, defects, and internal stresses.⁷

Recent experimental studies show that internal stresses have a great impact on the dielectric behavior of BST thin films.^{3,8–11} Significant variations in the dielectric constant close to an order of magnitude have been observed in epitaxial BST thin films for which the internal stress levels were systematically altered either by using different substrate materials or by adjusting the film thickness.^{3,8,9} Experimental

results also indicate that the tunability of BST films displays a strong dependence on the lattice misfit, or the misfit strain.^{3,11,12} For example, it was shown that annealing treatments to reduce residual stresses in $\text{Ba}_{0.4}\text{Sr}_{0.6}\text{TiO}_3$ films would improve the tunability from 36% to 52% for a 57 kV/cm field on “compressive” LaAlO_3 substrate (i.e., substrate with lattice parameters smaller than the film such that compressive stresses are induced in the plane of the film–substrate interface in pseudomorphic films) but reduce the tunability from 47% to 38% on “tensile” MgO substrate.¹² A remarkable increase of the tunability from 20% to 32% for a 40 kV/cm field was reported for $\text{Ba}_{0.35}\text{Sr}_{0.65}\text{TiO}_3$ films on LaAlO_3 substrates after an annealing treatment.¹¹

The dependence of the structural, electrical, and electromechanical properties on the misfit strain in epitaxial ferroelectric films has been established theoretically via phenomenological models.^{3,8,9,13,14} However, the tunability, a parameter of both theoretical and practical importance in BST films, has not received a thorough treatment in theoretical work. In a very recent publication, we have developed misfit strain–temperature phase diagrams of epitaxial BST films¹⁴ taking into account the possibility of the formation of “unusual” phases that cannot form in bulk BST ceramics or single crystals by using a Landau–Devonshire (LD) phenomenology.¹³

Theoretical estimation of the dielectric constant of (001) $\text{Ba}_{0.7}\text{Sr}_{0.3}\text{TiO}_3$ and $\text{Ba}_{0.6}\text{Sr}_{0.4}\text{TiO}_3$ films on (001) Si, MgO, LaAlO_3 , and SrTiO_3 substrates as a function of misfit strain and film thickness was provided. An order-of-magnitude increase in the dielectric constant for films on LaAlO_3 and SrTiO_3 substrates with increasing film thickness was predicted. Due to the interplay between the relaxation of epitaxial stresses at the deposition temperature and the thermal

^{a)} Author to whom correspondence should be addressed; electronic mail: p.alpay@ims.uconn.edu

stresses between the film and the substrate that develop as the film is cooled down from the growth temperature, for films on MgO substrates the dielectric response is expected to increase as the film thickness decrease, attaining a maximum at around 40 nm.

In this article, we employ a similar treatment to analyze the tunability of epitaxial BST films taking into account the dependence of the dielectric response on the applied electric field. Our goal is to provide a quantitative estimation for the dependence of the tunability on epitaxy-induced internal stresses. In Sec. II, the thermodynamic model is provided. In Sec. III we calculate the dependence of the dielectric response on the applied electric field of $\text{Ba}_{0.5}\text{Sr}_{0.5}\text{TiO}_3$ (BST 50/50) films on various (001) cubic substrates as a function of the misfit strain. The tunability of BST 50/50 films is evaluated and compared with the experimental data reported

in the literature in Sec. III. The tunability as a function of film thickness is also presented for various substrates by taking into consideration the possibility of relaxation of epitaxial stresses through the formation of misfit dislocations at the film growth stage.

II. PHENOMENOLOGICAL MODEL

We consider a single-domain (001) BST film epitaxially grown in the cubic paraelectric state on a thick (001) cubic substrate. The thermodynamic potential \tilde{G} of a pseudocubic BST film as a function of polarization P_i , applied field E_i , and misfit strain $u_m = (a_s - a_0)/a_s$, where a_s is the substrate lattice parameter and a_0 is the cubic cell constant of the free standing film, is given by^{13,14}

$$\begin{aligned} \tilde{G} = & a_1^*(P_1^2 + P_2^2) + a_3^*P_3^2 + a_{11}^*(P_1^4 + P_2^4) + a_{33}^*P_3^4 + a_{13}^*(P_1^2P_3^2 + P_2^2P_3^2) + a_{12}^*P_1^2P_2^2 + a_{111}(P_1^6 + P_2^6 + P_3^6) \\ & + a_{112}[P_1^4(P_2^2 + P_3^2) + P_3^4(P_1^2 + P_2^2) + P_2^4(P_1^2 + P_3^2)] + a_{123}P_1^2P_2^2P_3^2 + \frac{u_m^2}{S_{11} + S_{12}}(E_1P_1 + E_2P_2 + E_3P_3). \end{aligned} \quad (1)$$

The vector and tensor quantities are defined in a Cartesian coordinate system as shown in Fig. 1 such that for example, $P_1 // [100]$, $P_2 // [010]$, and $P_3 // [001]$. The renormalized coefficients of the free energy expansion are

$$\begin{aligned} a_1^* &= a_1 - u_m \frac{Q_{11} + Q_{12}}{S_{11} + S_{12}}, \quad a_3^* = a_1 - u_m \frac{2Q_{12}}{S_{11} + S_{12}}, \\ a_{11}^* &= a_{11} + \frac{1}{2} \frac{1}{S_{11}^2 - S_{12}^2} [(Q_{11}^2 + Q_{12}^2)S_{11} - 2Q_{11}Q_{12}S_{12}], \\ a_{33}^* &= a_{11} + \frac{Q_{12}^2}{S_{11} + S_{12}}, \\ a_{12}^* &= a_{12} - \frac{1}{S_{11}^2 - S_{12}^2} [(Q_{11}^2 + Q_{12}^2)S_{12} - 2Q_{11}Q_{12}S_{11}] \\ & \quad + \frac{Q_{44}^2}{2S_{44}}, \\ a_{13}^* &= a_{12} + \frac{Q_{12}(Q_{11} + Q_{12})}{S_{11} + S_{12}}, \end{aligned} \quad (2)$$

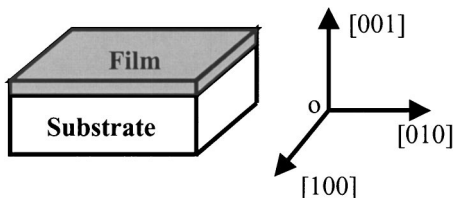


FIG. 1. Definition of the crystallographic directions with respect to the film and the substrate.

where a_1 is the dielectric stiffness, a_{ij} and a_{ijk} are higher order stiffness coefficients at constant stress, Q_{ij} are the electrostrictive coefficients, and S_{ij} the elastic compliances of the film. The temperature dependence of the dielectric stiffness a_1 is given by the Curie–Weiss law, $a_1 = (T - T_0)/2\epsilon_0 C$, where T_0 and C are the Curie–Weiss temperature and constant of a bulk ferroelectric, respectively, and ϵ_0 is the permittivity of free space. The parameters used for the calculation of the renormalized coefficients for BST films are obtained by averaging the corresponding parameters of BaTiO_3 (BT) and SrTiO_3 as given in Table I.^{13,15–18} The contribution of sixth-order polarization terms to the free energy is neglected.¹⁹

The temperature–misfit strain phase diagram for epitaxial BST 50/50 films is shown in Fig. 2. The details of the construction of the phase diagram, which is essentially based on the possibility of rotation of the polarization vector with

TABLE I. The parameters for the calculation of the renormalized coefficients for BST 50/50 films. Data compiled from Refs. 13 and 15–18: (T_C : Curie temperature, C : Curie constant, a_{ij} : stiffness coefficients, S_{ij} : elastic compliances, Q_{ij} : electrostrictive coefficients).

Parameters	BST 50/50
Curie temperature T_C ($^\circ\text{C}$)	-23
Curie constant C (10^5 $^\circ\text{C}$)	1.15
a_{11} ($10^6 \text{m}^2/\text{C}^2$ F)	$1.87T + 740(T \text{ in } ^\circ\text{C})$
a_{12} ($10^8 \text{m}^5/\text{C}^2$ F)	8.75
S_{11} ($10^{-12} \text{m}^2/\text{N}$)	4.33
S_{12} ($10^{-12} \text{m}^2/\text{N}$)	-1.39
S_{44} ($10^{-12} \text{m}^2/\text{N}$)	5.01
Q_{11} (m^4/C^2)	0.1
Q_{12} (m^4/C^2)	-0.034
Q_{44} (m^4/C^2)	0.029

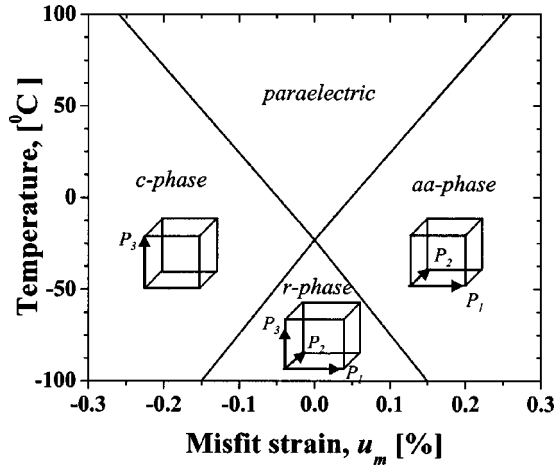


FIG. 2. Phase diagrams of single-domain epitaxial (001) BST 50/50 thin films on a (001) cubic substrate. Polarization components are indicated for the ferroelectric phases.

varying misfit strain, can be found elsewhere.^{13,14} The six possible phases identified by Pertsev *et al.*¹³ are the paraelectric phase, the *c* phase ($P_1=P_2=0, P_3 \neq 0$), the *a* phase ($P_1 \neq 0, P_2=P_3=0$), the *ac* phase ($P_1 \neq 0, P_2=0, P_3 \neq 0$), the *aa* phase ($P_1=P_2 \neq 0, P_3=0$) and the *r* phase ($P_1=P_2 \neq 0, P_3 \neq 0$).²⁰ Examination of Fig. 2 reveals that only the *c* phase, the paraelectric phase, and the *aa* phase are the stable phases for epitaxial BST 50/50 films at room temperature [(RT)=25 °C].

The polarization components as a function of the applied field can be obtained via $\partial \tilde{G} / \partial P_i = 0$ such that

$$\frac{\partial \tilde{G}}{\partial P_1} = 2(a_1^* + a_{13}^* P_3^2 + a_{12}^* P_2^2) P_1 + 4a_{11}^* P_1^3 - E_1 = 0, \quad (3)$$

$$\frac{\partial \tilde{G}}{\partial P_2} = 2(a_1^* + a_{13}^* P_3^2 + a_{12}^* P_1^2) P_2 + 4a_{11}^* P_2^3 - E_2 = 0, \quad (4)$$

$$\frac{\partial \tilde{G}}{\partial P_3} = 2[a_3^* + a_{13}^* (P_1^2 + P_2^2)] P_3 + 4a_{33}^* P_3^3 - E_3 = 0, \quad (5)$$

The electric field dependent relative dielectric constants along [001] and [100] directions can be determined by

$$\begin{aligned} \frac{\epsilon_{33}(E_3)}{\epsilon_0} &= \left(\epsilon_0 \frac{\partial^2 \tilde{G}}{\partial P_3^2} \right)^{-1} \\ &= \frac{1}{2\epsilon_0 [a_3^* + a_{13}^* (P_1^2 + P_2^2) + 6a_{33}^* P_3^2]} \end{aligned} \quad (6)$$

and

$$\begin{aligned} \frac{\epsilon_{11}(E_1)}{\epsilon_0} &= \left(\epsilon_0 \frac{\partial^2 \tilde{G}}{\partial P_1^2} \right)^{-1} \\ &= \frac{1}{2\epsilon_0 [a_1^* + a_{13}^* P_3^2 + (a_{12}^* + 6a_{11}^*) P_1^2]}, \end{aligned} \quad (7)$$

respectively. The small-signal dielectric response along [001] and [100] directions are also determined by Eqs. (6)–(7) with the polarizations given by setting E_i equal to zero in

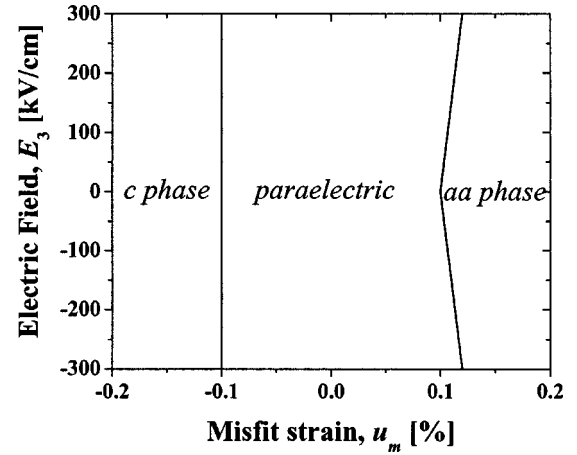


FIG. 3. The electric field E_3 —misfit strain phase diagram of BST 50/50 at RT.

Eqs. (3)–(5). We define the tunability Φ as the variation in the dielectric response with applied field with respect to the small-signal dielectric constant as¹¹

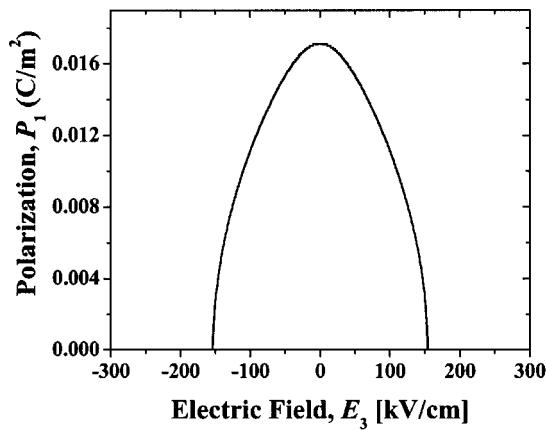
$$\Phi = \begin{cases} 1 - \epsilon_{33}(E_3) / \epsilon_{33}(E_3=0) & \text{for } E // [001] \\ 1 - \epsilon_{11}(E_1) / \epsilon_{11}(E_1=0) & \text{for } E // [100] \end{cases}. \quad (8)$$

III. RESULTS AND DISCUSSION

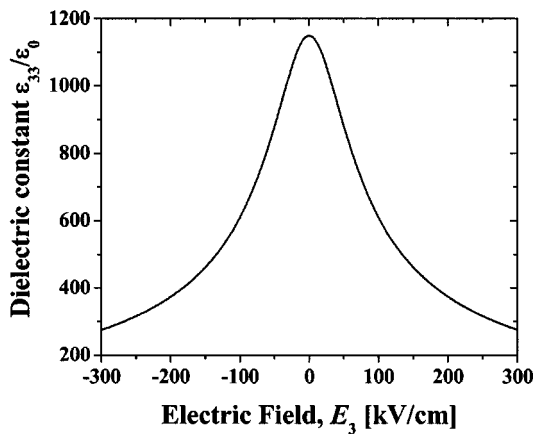
A. The dielectric response: effect of field

In order to study the dielectric response as a function of the applied electric field, the stability of the phases under the electric field has to be considered. To accomplish this, we calculate the minima of \tilde{G} [Eq. (1)] under an electric field E_3 normal to the film–substrate interface for all possible phases in an epitaxial BST 50/50 film. The resulting electric field–misfit strain phase diagram at RT is shown in Fig. 3. The stable phases in the range examined are the *c* phase, *paraelectric* phase, and the *aa* phase. At zero bias, the misfit strain range at which each phase is stable agrees with that obtained from the temperature–misfit strain phase diagram (Fig. 2). Close examination of Fig. 3 reveals that the electric field within the range considered has a minor effect on the stability of the phases. The application of the electric field does not affect the stability of the *c* phase and *paraelectric* phase. It should be noted that the misfit-driven transition from *c* phase to *paraelectric* phase is blurred in the presence of a nonzero electric field E_3 . However, the transition can be defined by the polarization versus electric field hysteresis characteristics of the phases.²¹ For $E_3 \neq 0$, the epitaxial film should exhibit a well-defined hysteresis loop when the misfit strain $u_m < -0.1$ while the hysteresis loop should not persist when $u_m > 0.1$.

However, the stability of the *aa* phase characterized by the in-plane polarizations $P_1=P_2$ shows, to some extent, a sensitivity to the external electric field E_3 . The progressive increase of the polarization P_3 induced by E_3 is concurrent with the decrease of the in-plane polarizations due to the coupling effect between P_3 and the in-plane polarizations. When the misfit strain is slightly higher than 0.1%, the *aa* phase has weak in-plane polarization components. As a re-



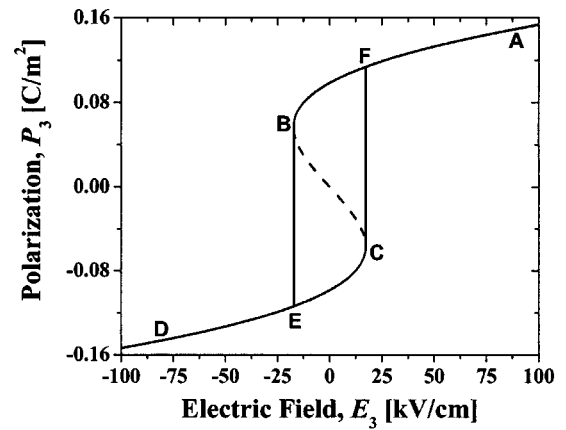
(a)



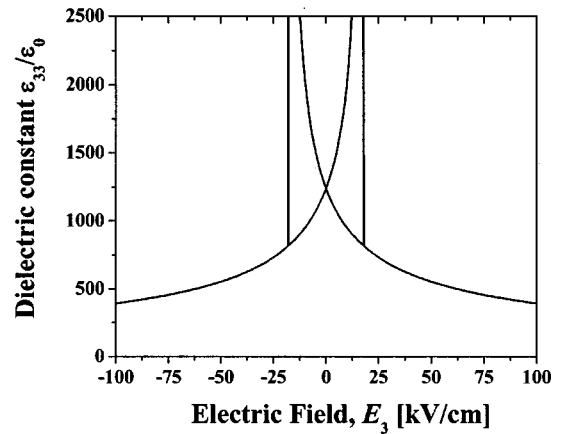
(b)

FIG. 4. The variation of in-plane polarization P_1 (a) and the relative dielectric constants ϵ_{33}/ϵ_0 (b) as a function of the electric field E_3 for the aa phase at the misfit strain $u_m=0.11\%$.

sult, the induced polarization P_3 may lead to the disappearance of the in-plane polarization at some critical electric field, thereby initiating a transition from the aa phase to the *paraelectric* phase. The instability of in-plane polarizations of the aa phase is presented in Fig. 4(a) which plots the variation of the in-plane polarization $P_1 (=P_2)$ as a function of E_3 at a misfit strain $u_m=0.11\%$. Figure 4(a) shows that the in-plane polarization $P_1 (=P_2)$ drops to zero in a continuous fashion with the increase of the applied field displaying a transition from the aa phase to *paraelectric* phase at a field ~ 150 kV/cm. The instability of the in-plane polarization in the presence of the electric field is also expected for the transition from the r phase to the c phase induced by the electric field (not shown in Fig. 3). The r phase ($P_1=P_2 \neq 0, P_3 \neq 0$) is stable below -25°C within a particular misfit strain range (see Fig. 2). When an electric field is applied along [001] which is parallel with P_3 , the in-plane polarizations will decrease. In other words, a rotation of the polarization vector toward the [001] direction in r phase is expected with an increase in the electric field. At sufficiently large electric fields, the diminishing in-plane polarizations P_1 and P_2 of the r phase eventually lead to a transition (with same characteristics as the c phase to *paraelectric* phase



(a)



(b)

FIG. 5. The variation of the polarization P_3 (a) and the relative dielectric constants ϵ_{33}/ϵ_0 (b) as a function of the electric field E_3 for the c phase at the misfit strain $u_m=-0.2\%$.

transition) to the c phase. Similar behavior in BaTiO_3 crystals has been reported where it was shown experimentally that phase transformations from rhombohedral to orthorhombic and to tetragonal phases could be induced by applying a significantly large field.²² Theoretical treatment of the phase transformations induced by an applied electric field in a stress-free ferroelectric BaTiO_3 system using the LD phenomenology model was also performed.²³

Using Eqs. (3)–(7), we plot the relative dielectric constants ϵ_{33}/ϵ_0 of BST 50/50 as a function of E_3 for films in the aa phase stability region [$u_m=0.11\%$, Fig. 4(b)] and for films in the c phase stability region [$u_m=-0.2\%$, Fig. 5(b)]. The relative dielectric constant versus the electric field behavior of the c phase exhibits remarkable differences with that of the aa phase. For the c phase, the dependence of ϵ_{33}/ϵ_0 on E_3 is characterized by two peaks positioned symmetrically with respect to zero field as shown in Fig. 5(b). The hysteresis in the dielectric constant as a function of applied field in forward and reverse electric field sweeps has been widely observed experimentally in $\text{Ba}_x\text{Sr}_{1-x}\text{TiO}_3$ ($x=0.4-0.7$) thin films under various conditions.^{12,24-26} The hysteretic behavior in the dielectric constant as a function of

the applied field is associated with polarization switching. The theoretical P_3 - E_3 hysteresis loop shown in Fig. 5(a) plotted using Eq. (5) displays typical ferroelectric characteristics. A coercive field around 20 kV/cm for the c phase at the misfit strain $u_m = -0.2\%$ is predicted in our model. It should be noted that the coercive fields calculated via phenomenological approaches are usually 1 or 2 orders of magnitude larger than the typically observed values. This is because of the fact that switching in thermodynamic treatments is due to instability of the polarization with respect to an applied field in the reverse direction rather than the nucleation and growth of 180° domains.²⁷

The relative dielectric constant ϵ_{33}/ϵ_0 as a function of E_3 for the aa phase at $u_m = 0.11\%$ is shown in Fig. 4(b). The dielectric constant dependence on the electric field for the *paraelectric* phase is not included because it behaves in a fashion similar to the aa phase. Since there is no spontaneous polarization along the [001] direction for the aa phase, the relationship between ϵ_{33}/ϵ_0 and E_3 with no hysteresis characteristics is expected. This expectation is justified in Fig. 4(b), which features a single peak at zero bias. With the increase of magnitude of the electric field, the relative dielectric constant decrease from its maximum value. It is interesting to note that the phase transformation from the aa phase to *paraelectric* phase induced by the applied electric field E_3 has no influence on the behavior of the dielectric constant dependence on the electric field. A continuous transition of the dielectric constant is predicted when the phase transformation from the aa phase to *paraelectric* phase occurs.

B. Tunability

The RT tunability of BST 50/50 thin film along [001] and [100] with applied fields along the same directions are calculated by using the definition of the tunability [Eq. (8)] and the dielectric response as a function of the applied field [Eqs. (6) and (7)]. The maximum applied field is taken as 67 and 40 kV/cm for $E//[001]$ and $E//[100]$, respectively and the results are presented in Figs. 6(a) and 6(b) for the two cases. Superimposed on these curves are the stability regions of the phases in accordance with the temperature–misfit strain (Fig. 2) and electric field–misfit strain (Fig. 3) phase diagrams. It is worth mentioning that the definition of the tunability in this article in essence reflects the variation of the dielectric permittivity with the maximum external electric field and is the most convenient measure adopted experimentally. A new definition of tunability, i.e., $\Phi = (\partial\epsilon_{ij}/\partial E_i)_{\max}$, was recently suggested.⁹ This definition corresponds to the maximum slope of the dielectric constant versus the applied field and is electric field independent. It is best suited to the case where there is no hysteresis [e.g., Fig. 4(b)]. Tunability defined in this way, however, always goes to infinity for a ferroelectric phase displaying hysteresis [e.g., Fig. 5(b)]. Therefore, it cannot capture the full characteristics of the phases predicted in our model. Furthermore, experimental data usually are presented in accordance with Eq. (8). Adopting Eq. (8) as to describe tunability enables us to compare our calculations with the available experimental data.

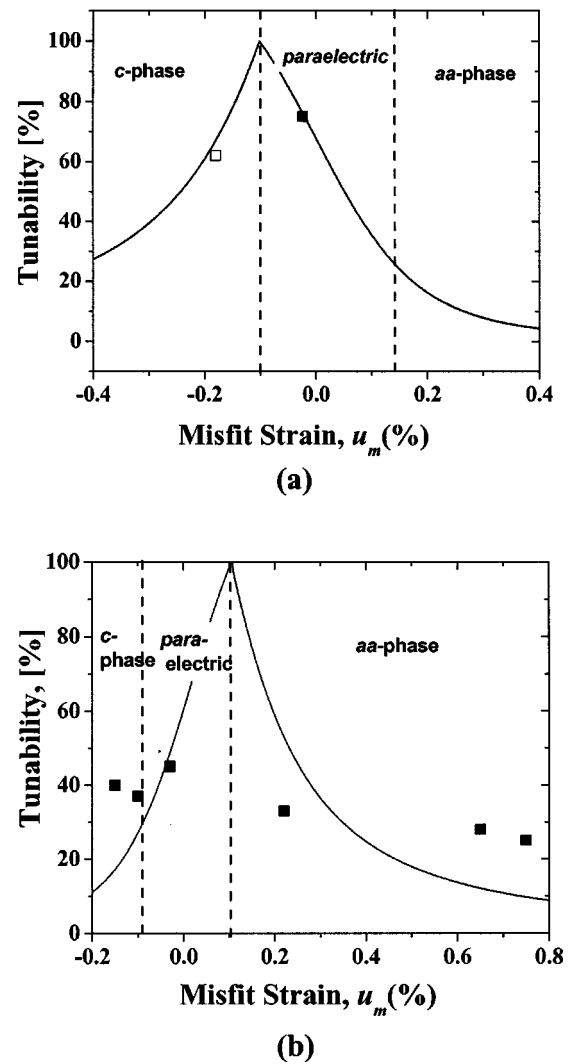


FIG. 6. The variation of the tunability along [001] (a) and [100] (b) as a function of the misfit strain in BST 50/50 epitaxial thin films at RT. The open and solid squares in (a) are experimental data from Ref. 3 and the solid squares in (b) are experimental data from Ref. 9 defining the tunability as $[\epsilon_{33}(0) - \epsilon_{33}(67 \text{ kV/cm})]/\epsilon_{33}(0)$ and $[\epsilon_{11}(0) - \epsilon_{11}(40 \text{ kV/cm})]/\epsilon_{11}(0)$ for (a) and (b), respectively.

Figures 6(a) and 6(b) show that the tunability is strongly dependent on the misfit strain. They indicate that theoretically maximum tunability can be attained at critical misfit strains corresponding to structural phase transformations and with either decrease or increase in the misfit strain a degradation of the tunability is expected. Interestingly, the stress-free condition does not result in maximum tunability. The critical misfit strain at which maximum tunability is achievable depends upon the direction of the applied electric field. Quantitatively, a maximum in the tunability is reached for $u_m = -0.1\%$ and for $u_m = 0.1\%$ for an applied field along [001] and [100], respectively. Referring back to the phase diagrams in Figs. 2 and 3, these critical misfit strains correspond to the transformation from the *paraelectric* phase to the c phase for an applied field along [001] and the transformation from *paraelectric* phase to the aa phase for an applied field along [100]. The tunability as well as the dielectric constant display similar behavior as a function of the

misfit strain¹⁴ indicating that both properties can be optimized via epitaxy-induced internal stresses.

The theoretical prediction of the tunability for BST 50/50 film may be compared with the limited experimental results published in the literature, as illustrated in Fig. 6. The two experimental points in Fig. 6(a) are for epitaxial BST 50/50 films with thickness ~ 500 nm grown at 750 °C in an oxygen ambient pressure of 350 mTorr on LaAlO₃ (solid square) and MgO substrates (open square) by pulsed laser deposition (PLD).³ Experimental data in Fig. 6(b) were obtained by Li *et al.*⁹ who investigated the effect of lattice misfit on the dielectric properties as well as the tunability of (001) 14–500 nm thick BST 50/50 films grown on MgO substrates by PLD with the substrate temperature held at 800 °C during deposition and a dynamic pressure of 120 mTorr O₂ established in the chamber. As the film thickness increases, internal stresses due to epitaxy are replaced by formation of misfit dislocations during the growth stage, resulting in a systematic variation of the misfit strain measured by x-ray diffraction methods. Several points enter the compressive strain region owing to the difference in the thermal expansion coefficients of the film and the substrate as the film is cooled down. It can be seen from Fig. 6 that the theoretical calculations of the effect of lattice misfit on the tunability are in good agreement with the experimental results.

C. Effect of film thickness

Obviously, the misfit strain in the heteroepitaxial films can be modified by the selection of a substrate material. Furthermore, systematic variations in the internal stress level of heteroepitaxial films can be achieved by altering the film thickness. The epitaxial stresses can be relaxed to a certain extent by the formation of misfit dislocations at the deposition temperature T_G depending on the thickness of the deposit.^{28–31} The degree of the relaxation is characterized by an effective misfit strain $u_m(T_G) = u_m^0$ at T_G that depends on the ratio of the critical thickness for misfit dislocation formation h_ρ and the film thickness h via

$$u_m^0 = \rho a_0(T_G) \left(1 - \frac{h_\rho}{h} \right)^{-1}, \quad (9)$$

where ρ is the equilibrium liner misfit dislocation density at T_G . Assuming no additional dislocations form during cooling down [i.e., $\rho(T_G) = \rho(T)$ for $T < T_G$], an “effective” substrate lattice parameter \bar{a}_S can be defined and used for the calculation of the misfit strain of the films with different thickness grown on a selected substrate^{31,32}

$$\bar{a}_S(T) = \frac{a_S(T)}{\rho a_S(T) + 1}. \quad (10)$$

We have recently provided a theoretical estimation correlating the film thickness to the misfit strain for BST films on “compressive” substrates such as SrTiO₃ (STO) and LaAlO₃ (LAO) and “tensile” substrates such as Si and MgO.¹⁴

Using the “effective” substrate lattice parameter concept, the dependence of the tunability on the film thickness can be established. Figures 7(a)–7(c) plot the dependence of

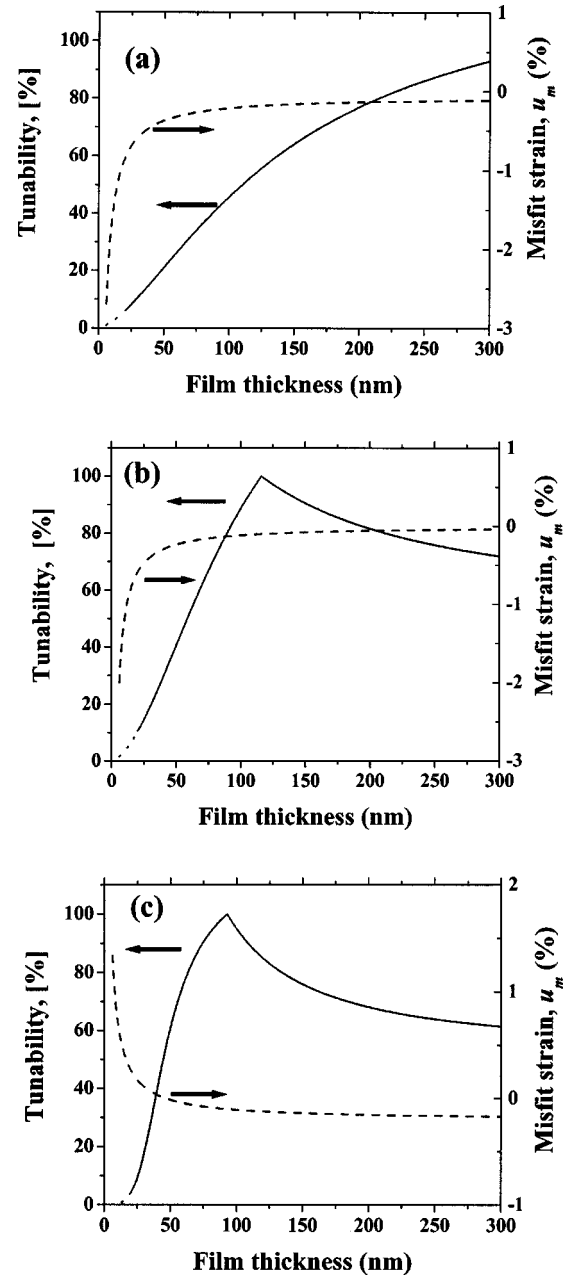


FIG. 7. The dependence of tunability along [001] (solid lines) and misfit strain (dashed lines) on film thickness for BST 50/50 epitaxial thin films on various substrates at RT: (a) STO, (b) LAO, and (c) MgO.

the tunability on the film thickness for BST 50/50 on STO, LAO, and MgO substrates at RT for an applied field along [001] assuming that T_G is 800 °C. The critical thickness for dislocation formation on STO, LAO, and MgO are calculated to be approximately 19.6, 2.8, and 1.4 nm, respectively, using the Matthews–Blakeslee criteria.^{31,33} The variation in the misfit strain as a function of the film thickness for the three substrates is also included in Figs. 7(a)–7(c) (dashed lines). Note that in-plane compressive stresses are developed on MgO substrate for films thicker than 45 nm due to the interplay between the misfit dislocation generation at T_G and the thermal stresses due to the difference in the thermal expansion coefficients of the film and the substrate that develop as the film cools down from T_G . It should be pointed out that

the misfit strain for (001) films on (001) Si substrate as high as 1.0% is predicted even by taking into account the relaxation due to formation of the misfit dislocations at T_G ¹⁴ and the resulting tunability is less than 1% for a maximum applied field of 67 kV/cm. Noticeable tunability can only be achieved at extremely high fields (>100 kV/cm). This agrees with the experimental data reported by Basceri *et al.*³⁴ In practice, one or more buffer layers between the film and substrate are often used to reduce the internal stresses in the film.²⁶

It can be seen from Fig. 7(a) that the tunability of the film on STO substrate increases continuously with increasing film thickness. This is due to the fact that the film on STO remains in the c phase region throughout the thickness range evaluated. Therefore, films on STO substrates should be as thick as possible in order to achieve optimum tunability. For films on the MgO and LAO substrates, however, the tunability behaves significantly different. There is a maximum in the tunability at ~ 120 and 90 nm for films on LAO and MgO substrates, respectively. The tunability drops off sharply for films with a thickness less than the critical value. The rate of decline in the tunability is relatively smaller for films thicker than the critical thickness. The maximum in the tunability is associated with a phase transformation from the c phase to the *paraelectric* phase due to the reduction in the magnitude of the misfit strain with increasing film thickness [see Fig. 6(a)]. Consequently, to obtain maximum tunability, the thickness of BST 50/50 films on MgO and LAO substrates should be chosen as close to the critical film thickness as possible.

IV. CONCLUDING REMARKS

We have developed a thermodynamic model based on the LD phenomenology to provide a quantitative prediction of the tunability in epitaxial BST films on various substrates as a function of film thickness. We have shown that the selection of the substrate and/or the film thickness can be chosen as design parameters to manipulate the strain state in the film to achieve optimum tunability. The analysis is in good agreement with experimental results and explains the general trend observed in experimental studies that show that the tunability significantly deteriorates with increasing internal stress level.^{11,12} Annealing treatments as well as the deposition of a buffer layer is generally used to lower the internal stress level as to improve the tunability in ferroelectric thin films.

Although we have focused on the BST 50/50 composition, the approach can be readily applied to other BST compositions with only slight modifications. For compositions close to STO, it should be taken into account that upon cooling bulk STO undergoes a cubic to tetragonal antiferrodistortive transition at 105 K. A ferroelectric transformation in stress-free STO crystals is not observed but it is possible to induce ferroelectricity via external^{35,36} as well as internal stresses due to epitaxy.¹⁶

It is worthwhile to note some limitations of the model employed. First of all, the coefficients in the free energy expansion for BST film are obtained by simply averaging the

corresponding free energy expansion coefficients and the elastic moduli of BT and STO due to lack of data on single crystals of the same composition. Second, the sixth-order polarization terms and their coupling with internal stresses are neglected, which is a reasonable approximation in the vicinity of T_C .³⁷ Furthermore, we have disregarded the possibility of the formation of polydomain (polytwin) structures as a mechanism to relax internal stresses because of the small self-strain of the paraelectric–ferroelectric phase transformation in the investigated temperature range. Although the formation of certain polydomain structures is thermodynamically possible for relatively large tensile misfits,^{31,33,38–45} there is no experimental observation of such structures in epitaxial BST films with Ba concentration in the 0.3–0.7 interval. Additionally, it should be kept in mind that the misfit dislocation model of Matthews and Blakeslee is the result of a thermodynamic analysis and thus the real critical thickness for dislocation formation and the linear equilibrium dislocation density may differ significantly from the actual observed values because of kinetic factors.^{30,46,47} A variation in the critical thickness for misfit dislocation generation should in turn alter the critical thickness for maximum tunability [Fig. 7(b) and 7(c)] but not the value of the critical misfit strain (Fig. 6). Finally, the thermodynamic model may not be applicable for films less than ~ 20 nm thick because the model does not take into account depolarizing fields and surface effects, which may tend to suppress ferroelectricity.^{7,48–50} Very recently, it was proposed that the so-called size effect in ferroelectric particles is due to a decrease in the spontaneous polarization at the particle core instead of the surface effect or the depolarization fields.⁵¹ The phenomenological treatment showed that the LD expansion coefficients may very well be size dependent.

As a final note, a tunability as high as 100% is predicted for epitaxial BST films in our calculations close to the critical misfit. Experimentally, only a tunability of $\sim 80\%$ has been reported.³ This discrepancy is mainly because of the overestimation of the small-signal dielectric constant that displays an anomaly at the critical misfit strain due to the structural phase transformations, resulting in a very high tunability in the vicinity of the critical misfit. However, such a sharp response in the dielectric constant as a function of temperature in actual films cannot be observed mainly due to microstructural and chemical inhomogeneities as well as defects which tend to diffuse the paraelectric–ferroelectric phase transformation over a temperature interval rather than a single point. Far from the critical strain, however, our calculations are in good agreement with the experimental data from the literature.

ACKNOWLEDGMENTS

The support from the National Science Foundation (NSF) under Grant No. DMR-0132918 and the University of Connecticut Research Foundation are gratefully acknowledged. The authors also would like to thank M. Aindow (University of Connecticut) and A. L. Roytburd (University of Maryland) for many useful discussions.

- ¹S. Summerfelt, (Ba,Sr)TiO₃ *Thin Films for DRAM's*, in *Thin Film Ferroelectric Materials and Devices*, edited by R. Ramesh (Kluwer Academic, Boston, 1997), p. 1.
- ²A.I. Kingon, S. K. Streiffer, C. Basceri, and S. R. Summerfelt, *Mater. Res. Bull.* **21**, 46 (1996).
- ³W. Chang, C. M. Gilmore, W.-J. Kim, J. M. Pond, S. W. Kirchoefer, S. B. Qadri, D. B. Chrisey, and J. S. Horwitz, *J. Appl. Phys.* **87**, 3044 (2000).
- ⁴J. Im, O. Auciello, P. K. Baumann, S. K. Streiffer, D. Y. Kaufman, and A. R. Krauss, *Appl. Phys. Lett.* **76**, 625 (2000).
- ⁵C. L. Chen *et al.*, *Appl. Phys. Lett.* **78**, 652 (2001).
- ⁶H.-D. Wu, Z. Zhang, F. Barnes, C. M. Jackson, A. Kain, and J. D. Cuchiaro, *IEEE Trans. Appl. Supercond.* **4**, 156 (1994).
- ⁷T. M. Shaw, S. Trolrier-McKinstry, and P. C. McIntyre, *Annu. Rev. Mater. Sci.* **30**, 263 (2000).
- ⁸C. L. Canedy, H. Li, S. P. Alpay, L. Salamanca-Riba, A. L. Roytburd, and R. Ramesh, *Appl. Phys. Lett.* **77**, 1695 (2000).
- ⁹H. Li, A. L. Roytburd, S. P. Alpay, T. D. Tran, L. Salamanca-Riba, and R. Ramesh, *Appl. Phys. Lett.* **78**, 2354 (2001).
- ¹⁰T. M. Shaw, Z. Suo, M. Huang, E. Liniger, R. B. Laibowitz, and J. D. Baniecki, *Appl. Phys. Lett.* **75**, 2129 (1999).
- ¹¹L. A. Knauss, J. M. Pond, J. S. Horwitz, D. B. Chrisey, C. H. Mueller, and R. Treece, *Appl. Phys. Lett.* **69**, 25 (1996).
- ¹²C. M. Carlson, T. V. Rivikin, P. A. Parilla, J. D. Perkins, D. S. Ginley, A. B. Kozayev, V. N. Oshadchy, and A. S. Pavlov, *Appl. Phys. Lett.* **76**, 1920 (2000).
- ¹³N. A. Pertsev, A. G. Zembilgotov, and A. K. Tagantsev, *Phys. Rev. Lett.* **80**, 1988 (1998).
- ¹⁴Z.-G. Ban and S. P. Alpay, *J. Appl. Phys.* **91**, 9288 (2002).
- ¹⁵*Landolt-Börnstein, Numerical Data and Functional Relationships in Science and Technology*, edited by K.-H. Hellwege and A. M. Hellwege (Springer, Berlin, 1981), Vol. 16.
- ¹⁶N. A. Pertsev, A. K. Tagantsev, and N. Setter, *Phys. Rev. B* **61**, R825 (2000).
- ¹⁷T. Yamada, *J. Appl. Phys.* **43**, 328 (1972).
- ¹⁸A. D. Hilton and B. W. Ricketts, *J. Phys. D* **29**, 1321 (1996).
- ¹⁹M. E. Lines and A. M. Glass, *Macroscopic and Phenomenology*, in *Principles and Applications of Ferroelectrics and Related Materials*, edited by W. Marshall and D. H. Wilkinson (Clarendon, Oxford, 1977), p. 59.
- ²⁰It should be noted that these phases are in essence orientational variants of the tetragonal and the orthorhombic ferroelectric phases that are observed in bulk BaTiO₃ ceramics and single crystals in succession with decreasing temperature with the exception of the *r* phase. The *c* and *a* phases are tetragonal (space group *P4mm* No. 99), the *aa* and *ac* phases are orthorhombic (space group *Amm2*, No. 38), and the *r* phase is monoclinic (space group *Pm*, No. 6) compared to the rhombohedral phase with $P_1 = P_2 = P_3 \neq 0$ (space group *R3m*, No. 160).
- ²¹E. Fatuzzo and W. J. Merz, in *Thermodynamic Theory of Ferroelectrics*, in *Ferroelectricity*, edited by E. P. Wohlfarth (North-Holland, Amsterdam, 1967), p. 141.
- ²²O. E. Fesenko and V. S. Popov, *Ferroelectrics* **37**, 729 (1981).
- ²³A. J. Bell and L. E. Cross, *Ferroelectrics* **59**, 197 (1984).
- ²⁴B. H. Park, Y. Gim, Y. Fan, Z. X. Jia, and P. Lu, *Appl. Phys. Lett.* **77**, 2587 (2000).
- ²⁵K. Abe and S. Komatsu, *J. Appl. Phys.* **77**, 6461 (1995).
- ²⁶B. H. Park, E. J. Peterson, Q. X. Jia, J. Lee, W. Si, and X. X. Xi, *Appl. Phys. Lett.* **78**, 533 (2001).
- ²⁷F. Jona and G. Shirane, *Ferroelectric Crystals* (Dover, New York, 1962), p. 21.
- ²⁸J. H. van der Merve, *J. Appl. Phys.* **34**, 123 (1963).
- ²⁹J. W. Matthews and A. E. Blakeslee, *J. Cryst. Growth* **27**, 118 (1974).
- ³⁰W. D. Nix, *Metall. Trans. A* **20**, 2217 (1989).
- ³¹J. S. Speck and W. Pompe, *J. Appl. Phys.* **76**, 466 (1994).
- ³²S. P. Alpay, V. Nagarajan, A. Bendersky, M. D. Vaudin, S. Aggarwal, R. Ramesh, and A. L. Roytburd, *J. Appl. Phys.* **85**, 3271 (1999).
- ³³S. P. Alpay and A. L. Roytburd, *J. Appl. Phys.* **83**, 4714 (1998).
- ³⁴C. Basceri, S. Streiffer, A. I. Kingon, and R. Waser, *J. Appl. Phys.* **82**, 2497 (1997).
- ³⁵J. C. Slonczewski and H. Thomas, *Phys. Rev. B* **1**, 3599 (1970).
- ³⁶H. Uwe and T. Sakudo, *Phys. Rev. B* **13**, 271 (1976).
- ³⁷N. A. Pertsev, V. G. Koukhar, R. Waser, and S. Hoffmann, *Appl. Phys. Lett.* **77**, 2596 (2000).
- ³⁸J. S. Speck, A. C. Daykin, A. Seifert, A. E. Romanov, and W. Pompe, *J. Appl. Phys.* **78**, 1696 (1995).
- ³⁹N. A. Pertsev and A. G. Zembilgotov, *J. Appl. Phys.* **78**, 6170 (1995).
- ⁴⁰N. A. Pertsev and A. G. Zembilgotov, *J. Appl. Phys.* **80**, 6401 (1996).
- ⁴¹N. Sridhar, J. M. Rickman, and D. J. Srolovitz, *Acta Mater.* **44**, 4085 (1996).
- ⁴²N. Sridhar, J. M. Rickman, and D. J. Srolovitz, *Acta Mater.* **44**, 4097 (1996).
- ⁴³V. G. Koukhar, N. A. Pertsev, and R. Waser, *Phys. Rev. B* **64**, 214103 (2001).
- ⁴⁴B. S. Kwak, A. Erbil, J. D. Budai, M. F. Chrisholm, L. A. Boatner, and B. J. Wilkens, *Phys. Rev. B* **49**, 14865 (1994).
- ⁴⁵V. G. Koukhar, N. A. Pertsev, and R. Waser, *Phys. Rev. B* **64**, 214103 (2001).
- ⁴⁶L. B. Freund, *MRS Bull.* **17**, 52 (1992).
- ⁴⁷L. B. Freund and W. D. Nix, *Appl. Phys. Lett.* **69**, 173 (1996).
- ⁴⁸D. R. Tilley and B. Žekš, *Solid State Commun.* **49**, 823 (1984).
- ⁴⁹D. R. Zhong, Y. G. Wang, P. L. Zhang, and B. D. Qu, *Phys. Rev. B* **50**, 698 (1994).
- ⁵⁰B. Jiang and L. A. Bursill, *Phys. Rev. B* **60**, 9978 (1999).
- ⁵¹E. K. Akdogan and A. Safari, *J. Appl. Phys.* (in press).